

ERRATA SHEET

Page 6.4-3: 12th line

need left parenthesis for

(Kraner et al., 1964)

Page 6.4-5: lines 8 and 9 should read

K = ratio of gamma attenuation cross section in water to cross section in soil, taken to be unity;

*Reprinted from* **Advanced Concepts and Techniques in the Study of Snow and Ice Resources**  
ISBN 0-309-02235-5 NATIONAL ACADEMY OF SCIENCES Washington, D. C. 1974

NATURAL GAMMA SPECTRAL PEAK METHOD  
FOR SNOW MEASUREMENT FROM AIRCRAFT

Vernon C. Bissell  
NOAA, National Weather Service  
Silver Spring, Maryland 20910 U.S.A.

## ABSTRACT

The accuracy of airborne measurements of snow water equivalent over large areas using the  $^{40}\text{K}$  gamma radiation spectral peak is limited both by the accuracy of soil moisture estimates and by variation in general radon distributions between missions. The accuracy of the  $^{208}\text{Tl}$  spectral peak method is constrained only by soil moisture estimate accuracy and is therefore preferred over large areas. The use of an optimal linear combination of the  $^{40}\text{K}$  and  $^{208}\text{Tl}$  method water equivalent measurements significantly improves accuracy over small basins where only one or two flights are made.

To complement current literature on gamma snow surveys, dynamic aspects of radon in both soil and atmosphere are reviewed.

## INTRODUCTION

Recent studies have shown that airborne surveys of terrestrial gamma radiation can provide measurement of snow cover water equivalent with operational accuracy (Peck et al., 1971; Grasty, 1973; Burson and Fritzsche, 1972; Vershinina and Dimaksyan, 1969). Due to the difficulty of obtaining ground-based point measurements in windblown drifted snow fields, this method may be extremely valuable in obtaining water equivalent measurements more representative of areal conditions. The United States National Weather Service, in cooperation with EG&G, Inc., and the U.S. Atomic Energy Commission, has been conducting research in the method since 1969. Research missions have been conducted primarily at three lines. The first two are located just south of Luverne, Minnesota, while the third study line is in a level mountain valley near Steamboat Springs, Colorado. Another paper in this symposium (Jones et al., paper 6.2) reports many of the program results to date. This paper complements those results by discussing the composition of spectral peak errors, as well as reviewing some of the dynamic aspects of the natural radiation environment.

## THE DYNAMIC RADIATION ENVIRONMENT OF SNOW SURVEYS

The principal sources of count rates obtained with the ARMS detector system at 500 feet (152 m) altitude and their relative magnitudes are: (1.) radioactive decay of  $^{40}\text{K}$  in the ground and of  $^{238}\text{U}$  and  $^{232}\text{Th}$  and their decay products in ground and air (about 75%); (2.) cosmic radiation (about 15%); and (3.) the background of the aircraft and detector system itself (about 10%). The cosmic radiation flux is nearly constant in time at a given latitude, most variations being due to atmospheric pressure changes and time within the 11-year solar cycle. Neither the cosmic flux (slight variability) nor the aircraft and detector background (nearly constant) present major problems in the radiation method of snow surveys.

A major difficulty arises, however, from the variability of  $^{214}\text{Pb}$  and  $^{214}\text{Bi}$ , major gamma emitters in the  $^{238}\text{U}$  chain. These radioisotopes are decay products of  $^{222}\text{Rn}$ , a noble gas with a sufficiently long half-life to allow its transport from soil into the atmosphere in considerable quantities. While the name "radon" is generally reserved for the isotope  $^{222}\text{Rn}$ , there are two other isotopes of radon as well. The isotope  $^{219}\text{Rn}$  ("actinon") is relatively insignificant, whereas the isotope  $^{220}\text{Rn}$  ("thoron") is a parent atom of  $^{208}\text{Tl}$ , which produces the important gamma spectral peak at 2.62 MeV. The distance a radon atom may travel is limited by its life time. Radon gas ( $^{222}\text{Rn}$ ) has a half-life of about 3.8 days. Its range in the earth environment therefore is much greater than that of thoron, the half-life of which is only 52 seconds. The decay products of radon and thoron are heavy metals and are therefore immobile unless produced by decay in the atmosphere. Over 90% of the natural radioactivity in the atmosphere results from radon and its short-lived daughters (Shafrir et al., 1967).

The dynamics of radon distribution in the natural radiation environment involve three basic processes: (1.) transport of radon from soil particles into the soil water or soil air; (2.) transport of radon by and through the soil water or soil air; and (3.) the transport of radon and its subsequent decay products in the atmosphere. To illustrate the importance of these processes, Paul (1954) points out that the majority of gamma activity from uranium minerals comes from trapped radon and its decay products. The variable radon content in the upper soil layer then profoundly affects the gamma radiation flux over porous rocks and soil.

One of the most important steps of radon transport within a soil grain occurs at the instant of its formation (Tanner, 1964). All isotopes of radon are formed by the alpha decay of a radium isotope. When this occurs, the recoil atom's kinetic energy is dissipated along its path until it comes to rest, after which it either decays within the soil grain or diffuses through the grain into the soil interstices. Comparison of recoil path lengths in air, soil, and water points up two important phenomena: (1.) only a small fraction of the radon atoms will terminate their recoil paths in soil air, since the distance traveled per kinetic energy expended is much larger in air than in soil; (2.) moisture in the soil interstices will increase the fraction of recoil atoms escaping the soil particles, since the recoil range in water is much less than in air. Even if a decay atom comes to rest in a water-filled pore, its chances of escape into the atmosphere are greater than if it had stopped within a soil grain crystal because of the difference of diffusion constants in these materials (Tanner, 1964).

The total fraction of radon atoms which escape the mineral grains by either recoil or diffusion is known as the "emanating power" of the rock or soil. Emanating powers range from nearly nonexistent to 100% depending on the material with most measurements from 10 to 30 percent (Paul, 1954; Tanner, 1964).

Migration of radon isotopes through soil interstices can occur either by diffusion or convection. Diffusion is dominant in unsaturated undisturbed soil or unfractured rock, while in fractured rock or disturbed soil convection by soil air will dominate (Tanner, 1964). Also, radon can be convected to deeper soil layers by infiltrating water. Since the equilibrium ratio of radon concentration in water at 0°C to its concentration in air is roughly twice that at 25°C (Paul, 1954), this effect would be more important during the percolation of snowmelt water

than during summer rain. This phenomenon, combined with the attenuating effect of additional soil water, may cause spurious results from gamma snow measurements during periods of active melt.

The convection of radon by soil air can be produced by several phenomena: (1.) at the outset of a rain or snowmelt event the wetting surface of the percolating water moves downward, displacing radon-rich air upward as it goes (Tanner, 1964); (2.) a drop in barometric pressure results in expansion of radon-rich soil air, providing an upward displacement (Kraner et al., 1964); (3.) gusting winds provide a "pumping" action which draws radon-rich air out of the soil by a pressure gradient. As the gust dies down, diluted air replaces the soil air drawn out (Kraner et al., 1964).

Soil water and ice can significantly inhibit diffusion and convection of radon from the soil. A "capping" effect can occur in which precipitation (or snowmelt), freezing, or snow cover tend to seal the ground, thereby causing a buildup of radon in the uppermost soil layer. Perhaps the most revealing study of hydrologic and meteorological effects on radon in soil gas was conducted by Kovach (1945), who found the following: (1.) frozen ground produced the highest radon concentration. In fact, the depletion profile is practically eliminated during long periods of ice and snow coverage, causing the radon content at all depths to approach the same value; (2.) snow on the ground enhanced the content of radon in soil gas, but was not a greater influence than frozen ground; (3.) prolonged dry spells produced a very consistent profile of radon concentration from 25 to 150 cm depth; (4.) ground temperature changes apparently had no great effect on radon concentration in soil gas.

Capping by freezing depends not only on the fact that the ground is frozen, but also on the structure of the ice formed. Kraner et al. (1964) found that ground frozen to six inches (15.24 cm) depth or more still exhaled radon at 60% of the rate observed during summer. This fact might have important future application to river forecasters, to whom the permeability of frozen ground to rain or snowmelt water is extremely critical. Atmospheric radon levels may be a potential indicator of soil ice structure.

Radon exhalation rates encountered over agricultural areas will probably be larger than those in areas of undisturbed soils. Styra et al. (1970) found that thoron (<sup>220</sup>Rn) exhalation from a ground surface plowed to a twenty-centimeter depth is two or three times greater than that from smooth, bare, undisturbed ground.

Once radon escapes the soil surface, major influences producing its distribution in the atmosphere are the rate of atmospheric diffusion, transport by turbulent mixing (convection), transport by wind (advection), and "washout" by precipitation. Since radon comes from the ground, its concentration will be maximum at ground level. Transport to higher levels takes place mainly through eddy diffusion, which varies widely according to wind variation and atmospheric stability (Suschny, 1968). Under the normal decrease of temperature with altitude, transport of radon to higher levels is achieved quite easily. The presence of an inversion, however, blocks this transport and causes a buildup of radon below the inversion. This effect is magnified by the presence of snow cover. Peck and Bissell (1973) have pointed out this phenomenon as a major source of error in airborne gamma snow surveys.

The most marked characteristic of atmospheric radon is its diurnal fluctuation. The formation of low-level inversions during nocturnal

cooling of the earth's surface causes a buildup of radon which is depleted the following morning by increased convection and eddy diffusion as the inversion "burns out." An example of this effect is found in another paper in this symposium (Bissell and Peck, paper 6.3). The diurnal phenomenon would indicate that midday and afternoon aerial gamma snow surveys are preferred to early morning flights.

Work by Kirichenko (1970) perhaps best illustrates the variability of atmospheric radon. A ten-day sequence of vertical concentration profiles of radioactive aerosols showed sharp variations, most resulting from inversions at various altitudes. The natural radioactivity around noon at 200 m (roughly the altitude at which United States snow reconnaissance missions are expected) varied by a factor of ten for the ten days. The highest activity was observed under a strong inversion at 250 meters, while another extreme followed the passage of a warm front.

Another notable characteristic of atmospheric radon is its seasonal variation. Moses et al. (1963) found typically high values in summer and fall three feet (91 cm) above the ground at Argonne, Illinois. The highest monthly average for early morning concentration appeared in the late fall, probably due to the dry ground and reduced convection. Reduced exhalation from the soil due to occasional frozen ground and snow cover and from gradually increasing soil moisture caused atmospheric radon concentrations to decrease as fall progressed into winter. The minimum concentrations occurred in spring due to the combination of wet ground and strong gusty winds which rapidly mixed radon to higher levels. These results indicate that bare ground calibration flights for total-count snow reconnaissance should not be conducted during summer or dry fall weather.

The advection of radon-rich or radon-poor air into an area is a process which can produce rapid changes in local radon concentration (Kirichenko, 1970). Aircraft flights at 100 meters passing through cold fronts demonstrated that markedly high radioactivity is usually observed just ahead of a cold front. After the cold front passes, the radioactivity may be only about half that observed ahead of the front. This phenomenon was considered due to advection of radon-rich air away from the area, while rising pressure following the passage of the front inhibited exhalation of additional radon from the soil. Kirichenko also noted a second frontal passage effect in increased radioactivity following the passage of a warm front. Kirichenko suggested this phenomenon was due to radon "pumped" from the soil by the fluctuating unstable warm air mass behind the front.

All of the foregoing demonstrate that a radon-complicated gamma radiation spectrum is complicated indeed. Several methods for removal of airborne radon contributions to total count in snow surveys have been tried with varied degrees of success (Burson and Fritzsche, 1972), and research is continuing.

#### DETERMINATION OF SPECTRAL PEAK METHOD PARAMETERS

The  $^{40}\text{K}$  spectral peak is only moderately affected by radon daughter activity, while the  $^{208}\text{Tl}$  peak is unaffected. To use these peaks for water equivalent measurements then requires removal of cosmic and aircraft background from both peaks and removal of (radon daughter)  $^{214}\text{Bi}$  contributions from the  $^{40}\text{K}$  peak. On the basis of theoretical considerations,

and with a correction for soil moisture attenuation of gamma radiation (Fritzsche and Burson, 1970), the spectral peak count rate as a function of water equivalent is taken to be

$$N(W) = \frac{N_0}{1+KS} E_2(\alpha W) \quad (1)$$

where  $W$  = effective water equivalent, including air<sub>2</sub>blanket ( $\text{g}/\text{cm}^2$ );  
 $\alpha$  = mass attenuation coefficient in water ( $\text{cm}^2/\text{g}$ );  
 $S$  = soil moisture (fraction of dry weight);  
 $K$  = ratio of gamma attenuation cross section in water to cross section in air, taken to be unity;  
 $N_0$  = no-snow count rate with zero soil moisture;  
 $E_2$  = second order exponential integral function.

The actual peak count rates due to soil isotopes are computed from spectral window counts as

$$N_K = C_K - B_K + \beta_1 (C_B - B_B) + \beta_2 C_C$$

and

$$N_{Tl} = C_{Tl} - B_{Tl} + \gamma C_C$$

where  $C_K$  = count rate in <sup>40</sup>K spectral peak window;  
 $B_K$  = aircraft background in <sup>40</sup>K window;  
 $C_B$  = count rate in 1.76 MeV <sup>214</sup>Bi peak window;  
 $B_B$  = aircraft background in 1.76 MeV peak window;  
 $C_{Tl}$  = count rate in <sup>208</sup>Tl spectral peak window;  
 $B_{Tl}$  = aircraft background in <sup>208</sup>Tl peak window;  
 $C_C$  = count rate in high energy cosmic window;  
 $\beta_1, \beta_2, \gamma$  = "stripping coefficients."

The stripping coefficients allow removal of contributions to spectral peaks from radiation flux of higher energy, and are characteristic of the detector system. The mass attenuation coefficients are theoretically constants determined by the energy of the spectral peak, but in snow survey practice can vary somewhat between sites due to different radiation source geometry. Values of the mass attenuation coefficients  $\alpha$  and no-snow count rates  $N_0$  at each of the three survey lines were determined by a combination direct-search and regression which optimized the least-squares total of gamma-measured versus ground-measured water. The values of the detector stripping coefficients were determined simultaneously in the same optimization, and were in reasonable agreement with physical considerations. Removal of the <sup>208</sup>Tl contribution from the <sup>40</sup>K peak was not attempted since warping of the <sup>40</sup>K calibration curve to include this effect seemed preferable to the loss of statistical resolution which would result from such an attempt. For comparison, an exponential curve was used in a similar optimization with only slightly poorer results. The critical consideration in selection of a curve type, however, is which will perform best when water equivalent values are encountered outside the range of those used in the calibration period. For this reason, the  $E_2$  curve was chosen for further discussion on the basis of its theoretical justification. Table 1. summarizes the <sup>40</sup>K method results using an  $E_2$  curve.

Table 1. Optimization of results of  $E_2$  calibration curve values for  $^{40}\text{K}$  peak.<sup>2</sup>

Location	N (cts/min)	$\alpha$ ( $\text{cm}^2/\text{g}$ )	R.M.S. error (cm of water)
Steamboat Springs	14658	.0390	1.24
Luverne A	14256	.0428	0.56
Luverne W	15339	.0457	0.67

The estimated standard deviation in the data set, allowing eight degrees of freedom for parameter determinations, was 0.95 cm using the  $^{40}\text{K}$  peak and 1.03 cm using the  $^{208}\text{Tl}$  peak.

Table 2. Spectral stripping coefficients obtained by optimization of water measurements.

Curve type	$\beta_1$	$\beta_2$	$\gamma$
$E_2$	-1.16	-1.45	-1.75
Exponential	-1.14	-3.16	-2.55

The stripping coefficients determined are given in Table 2. The consistency of the  $^{214}\text{Bi}$  correction to the  $^{40}\text{K}$  peak between the two curve types is excellent. The poorer consistency of the cosmic stripping coefficients probably reflects both the use of the two different curves and the poor statistical quality of the cosmic window data used to derive the coefficients.

#### IDENTIFICATION OF RESIDUAL ERRORS

The determination of N and  $\alpha$  values ("calibration") of operational flight lines could take several years. Archiving water equivalent values with over-snow gamma counts would allow the "best" calibration curve parameters to be approached as time progresses. In the following error analysis curve-fitting errors are assumed negligible (this is reasonable since a large number of missions were used in parameter determination) and the method accuracy is taken to represent the long-term performance achievable. This approach complements the short-term (one calibration flight) error analysis given by Jones et al. (paper 6.2, this symposium).

A model II analysis of variance was used to separate the "within groups" errors from "between groups" errors. "Within groups" errors (those producing differences in measurement results between flights on the same day) were attributed to statistical count fluctuations in the spectral windows, rapid fluctuations in radon distributions, instrument calibration drift, flight navigation errors, and air mass calculation errors. The "between groups" errors (those producing a bias in all measurements on a given day, but a different and statistically independent bias on a different mission date) were attributed to soil moisture measurement errors, "ground truth" water equivalent measurement errors, changes in general radon distribution, and (since cosmic count rates were averaged over a mission date) the error in determining the cosmic radiation contribution. The resultant "within day" and "between day" errors are summarized in Table 3.

Table 3. Errors within days and between days from analysis of variance.

Measurement peak	"Within" error (cm)	"Between" error (cm)
$^{40}\text{K}$	.64	.67
$^{208}\text{Tl}$	.86	.53

A first order approximation using Equations 1.-3. of the water measurement variance due only to statistical count fluctuation showed this to be the dominant source of "within day" error. The relatively small remaining "within day" error (0.25 cm) was attributed, for convenience, to air blanket measurement errors. This assumption does not affect the error analysis in a substantive way. The breakdown of operational "within day" errors given in Table 4. assumes a detector volume identical to the ARMS detector, but assumes a cosmic spectral window wide enough that cosmic averaging over a day would not be necessary.

Table 4. Within-day errors ( $^{40}\text{K}/^{208}\text{Tl}$ ) with ARMS detector volume, wide cosmic window, and 2.5 minute counting time.

Effective water equivalent (snow plus air) in cm	Counting statistics (except cosmic) cm	Cosmic statistics cm	Air mass & others cm	Total cm
5-15	.20/.35	.01/.08	.25/.25	.32/.44
15-25	.37/.54	.03/.15	.25/.25	.45/.60
25-35	.63/.80	.04/.24	.25/.25	.68/.87
35-45	.98/1.17	.07/.39	.25/.25	1.01/1.26

The "between-day" errors encountered using the operational detector system assumed above would be only due to soil moisture estimate errors and general changes in the radiation source, and are given in Table 5.

Table 5. Between-day errors ( $^{40}\text{K}/^{208}\text{Tl}$ )

Std. dev. of soil moist. estimate	Soil moisture estimate (cm)	Radon and thoron variations (cm)	Total error (cm)
.02	.25/.23	.37/0	.45/.23
.05	.62/.58	.37/0	.72/.58
.07	.87/.81	.37/0	.95/.81
.10	1.17/1.12	.37/0	1.23/1.12

The effect of soil moisture error on water equivalent measurements was determined from Equation 1. The radon and thoron variation errors were determined as residuals after evaluating the errors common to both methods by correlating the  $^{40}\text{K}$  and  $^{208}\text{Tl}$  "between day" errors. The information in Tables 4. and 5. is combined in Figure 1. for the  $^{40}\text{K}$  peak method. The relative standard error (coefficient of variation  $C_V$ ) is shown in Figure 1. as well.

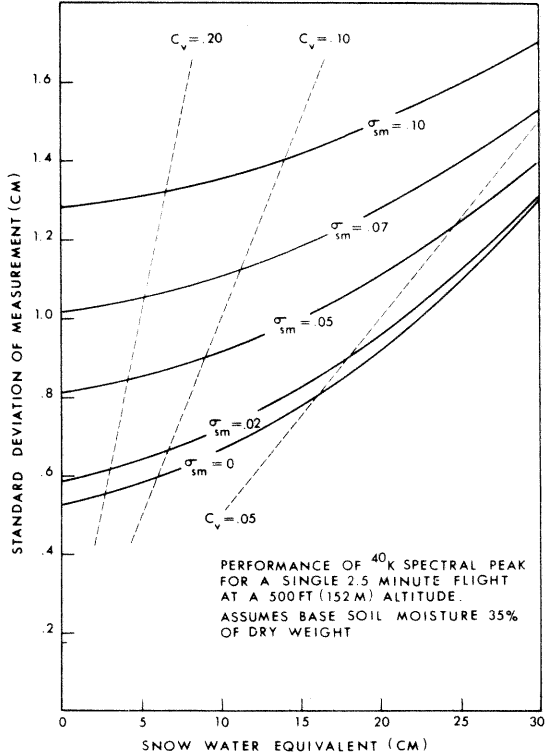


Figure 1. Single-flight accuracy of  $^{40}\text{K}$  peak. Assumes ARMS detector volume, wide cosmic window, and previous long-term calibration.

It is important in application to make best use of the water equivalent measurements in the two peaks. A weighted water equivalent estimate can be written as

$$W_F = F W_{40K} + (1-F) W_{208Tl} \quad (4)$$

An expression for the variance of  $W_F$  in terms of  $F$ , the errors determined previously and the number of flights over the line or basin on a given day was differentiated with respect to  $F$  and set to zero to determine the optimal linear combination. The optimal  $F$  values and resulting combination accuracy are shown as a function of the number of flights in Figure 2.

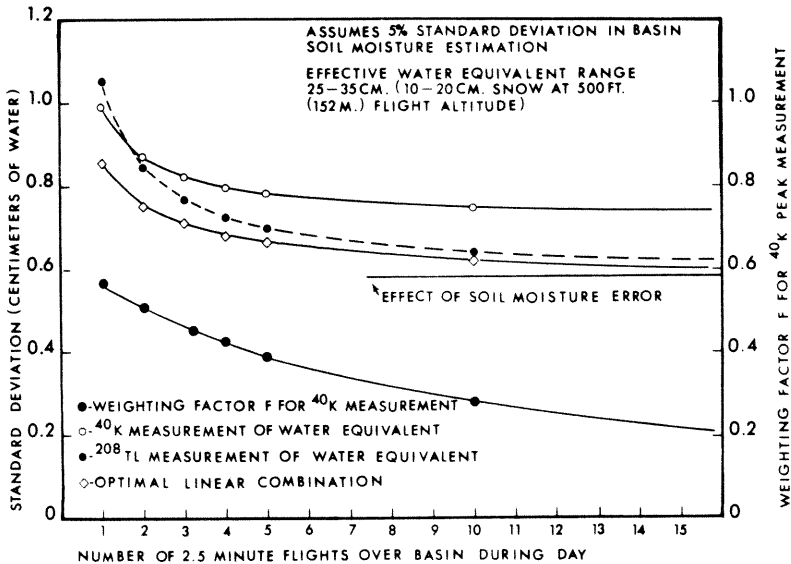


Figure 2. Performance of  $^{40}\text{K}$  and  $^{208}\text{Tl}$  spectral peaks.

The statistical quality of the  $^{40}\text{K}$  peak measurement dominates when only a few flights over a line or basin are made, but as the number of flights increases, the statistical error disappears. When many flights are used the  $^{208}\text{Tl}$  peak performance is superior to that of the  $^{40}\text{K}$  peak because it is subject only to basin soil moisture estimate error. The  $^{40}\text{K}$  peak is subject to general radon level bias as well. Thus, the optimal linear combination accuracy tends to the  $^{208}\text{Tl}$  peak accuracy which is ultimately constrained by surficial soil moisture estimate accuracy.

Finally, it should be noted that the above analysis only treats errors in snow measurement over selected lines. Basin water equivalent estimates are also subject to errors due to nonrepresentativeness of selected lines. Treatment of these network errors was not within the scope of this report.

#### REFERENCES

- Burson, Z. G., and A. E. Fritzsche, 1972. Snow Gaging by Airborne Radiological Surveys - Status Through September 1972. EGG-1183-1565, Tech. Rep. L-1078. EG&G, Inc., Las Vegas, Nevada. 48 pp.
- Faul, H., ed., 1954. Nuclear Geology, John Wiley and Sons, Inc., New York. pp. 138-143.
- Fritzsche, A. E., and Z. G. Burson, 1970. Water Equivalent of Snow Surveys. EGG 1183-1495. EG&G, Inc., Las Vegas, Nevada. 112 pp.

- Grasty, R. L., 1973. Snow-water Equivalent Measurement Using Natural Gamma Emission. *Nordic Hydrology*, 4. pp. 1-16.
- Kovach, E. M., 1945. Meteorological Influences Upon the Radon-content of Soil-gas. *Trans. Am. Geophys. U.*, Vol. 26, No. II. pp. 241-248.
- Kraner, H. W., G. L. Schroeder, and R. D. Evans, 1964. Measurements of the Effects of Atmospheric Variables on Radon-222 Flux and Soil-gas Concentrations. *The Natural Radiation Environment*. Adams, J.A.S., and W. M. Lowder, eds. Publ. for William Marsh Rice Univ. by U. of Chicago Press. pp. 191-215.
- Moses, H., H. F. Lucas, Jr., and G. A. Zerbe, 1963. The Effect of Meteorological Variables upon Radon Concentrations Three Feet Above the Ground. *Air Pollution Control Assoc. J.*, 13:12-19.
- Peck, E. L., V. C. Bissell, E. B. Jones, and D. L. Burge, 1971. Evaluation of Snow Water Equivalent by Airborne Measurement of Passive Terrestrial Gamma Radiation. *Water Resources Research*, 7(5). pp. 1151-1159.
- Peck, E. L. and V. C. Bissell, 1973. Aerial Measurement of Snow Water Equivalent by Terrestrial Gamma Radiation Survey. *Bull. of Int. Assoc. of Hydrol. Sci.*, XVIII, 1. pp. 47-62.
- Shafrir, U., G. Assaf, and M. Rindsberger, 1967. Possible Uses of Radioactive Isotopes for Meteorological Instrumentation. *Scient. Rep. No. 1, ESSA Agreement No. E-94-67(n)*, U.S. Dept. of Commerce. 32 pp.
- Styra, B. I., T. N. Nedveckaite and E. E. Senko, 1970. New Methods of Measuring Thoron (Radon 220) Exhalation. *J. Geophys. Res.*; 75(18). pp. 3635-3638.
- Suschny, O., 1968. The Measurement of Atmospheric Radioactivity. *Tech. Note No. 94*, World Meteorological Org., Geneva. 109 pp.
- Tanner, A. B., 1964. Radon Migration in the Ground: A Review. *The Natural Radiation Environment*. Adams, J. A. S., and W. M. Lowder, eds. Publ. for William Marsh Rice Univ. by U. of Chicago Press. pp. 161-190.
- Vershinina, L. K., and A. M. Dimaksyan, eds., 1969. Determination of the Water Equivalent of Snow Cover. Translated from Russian, Israel Program for Sci. Transl., TT70-50093, NTIS, Springfield, Va. 142 pp.

